Strangeness Signature of QGP

BNL, February 16, 2006

ABSTRACT: nucl-th/0602047, with Jean Letessier

We study the process of chemical equilibration of strangeness in dynamically evolving QGP fireball formed in relativistic heavy ion collisions at RHIC and LHC. We account for the contribution of direct and explore the thermal-QCD strangeness production mechanisms. The specific yield of strangeness per entropy is the primary target variable. We explore the effect of collision impact parameter, *i.e.*, fireball size, on strangeness chemical equilibration in QGP. Insights gained in study the RHIC data are applied to the study strangeness production at the LHC. We further consider how characteristic hadronic observables are influenced by the differences in the chemical equilibration, given a specific per entropy strangeness yield.**OBJECTIVES:**

1. **Introduction: nonequilibrium + statistical hadronization**
2. **Analysis and parameters for strangeness RHIC results (2xPRC, nucl-th/0412072,0506044)**
3. **Strangeness equilibration with fireball expansion**
4. **Centrality dependence of s/S at RHIC-200 and LHC**
5. **Soft strange hadrons at RHIC and LHC**

With Jean Letessier, Inga Kuznetsova, and Giorgio Torrieri, now Montreal

Supported by a grant from the U.S. Department of Energy, DE-FG02-04ER41318

Johann Rafelski
University of Arizona

1a. Chemical Non-equilibrium

INPUT: QGP fireball subject to rapid expansion, hadronization fast

Chemical potentials μ_i defined such that they control particle-antiparticle number difference e.g. baryon number,
Phase space occupancies γ_i defined such that they control sum of particle-antiparticle number that is pair yield.

We expect chemical nonequilibrium in final state $\gamma_i \neq 1$;
"Just an argument or is there some physics"?

- **Shift in hadron yields between**
  a) baryons and mesons: γ_q;
  b) strange and non-strange hadrons γ_s/γ_q;
  c) including relative yields of CHARMED HADRONS.
- **Strangeness oversaturation $\gamma_s^{\rm H} > 1$ is a diagnostic signature of deconfinement.**
- **Chemical non-equilibrium quark 'occupancy' γ_s can favor /disfavor onset of phase transition. What $\mu_{\rm B}$ can do, γ_i can do better as both quark and anti-quark number increase/decrease together.**

DISTINGUISH: hadron 'h' phase space and QGP phase parameters: micro-canonical variables such as baryon number, strangeness, charm, bottom, etc flavors are continuous, and entropy is almost continuous across phase boundary:

$$\gamma_s^{\rm QGP}\rho_{\rm eq}^{\rm QGP}V^{\rm QGP} = \gamma_s^{\rm h}\rho_{\rm eq}^{\rm h}V^{\rm h}$$

Equilibrium distributions are different in two phases and hence are densities:

$$\rho_{\rm eq}^{\rm QGP} = \int f_{\rm eq}^{\rm QGP}(p)dp \neq \rho_{\rm eq}^{\rm h} = \int f_{\rm eq}^{\rm h}(p)dp$$

We conclude: smooth across the phase boundary are the yields
strangeness, charm, entropy = multiplicity
and hence ratios, we will focus in this presentation on the observables:

$$\frac{s \text{ or } c}{S} = \frac{\text{number of valance strange, charm quark pairs}}{\text{multiplicity} = \text{entropy content in final state}}$$

And across any phase boundary when V does not adjust (and even in that case)

$$\gamma_s^{\rm QGP} \neq \gamma_s^{\rm h} \qquad \gamma_q^{\rm QGP} \neq \gamma_q^{\rm h}$$

Examples of what non-equilibrium parameters do

- $\tilde\gamma_s \equiv \gamma_s/\gamma_q$ **shifts the yield of strange vs non-strange hadrons:**

$$\text{the horn}: \frac{\rm K^+}{\pi^+} \propto \frac{\gamma_s^{\rm h}}{\gamma_q^{\rm h}}, \qquad \phi \text{ enhancement } \frac{\phi}{h} \propto \frac{\gamma_s^{\rm h\,2}}{\gamma_q^{\rm h\,2}},$$

$$\text{enhancement rise with strangeness number}: \frac{\Omega}{\Lambda} \propto \frac{\gamma_s^{\rm h\,2}}{\gamma_q^{\rm h\,2}},$$

- **For fixed $\tilde\gamma_s \equiv \gamma_s/\gamma_q$ and fixed other statistical parameters $(T, \lambda_i, \ldots)$:**

$$\frac{\text{baryons} \propto \gamma_q^{\rm h\,3}}{\text{mesons} \propto \gamma_q^{\rm h\,2}} \propto \gamma_q^{\rm h}\,.$$

HIGH ENTROPY STATE AND THE EXPECTED $\gamma_q^{\rm HG}$

QGP has excess of entropy, maximize entropy density at hadronization: $\boxed{\gamma_q^2 \to e^{m_\pi/T}}$**:**

Example:maximization of entropy density in pion gas $E_\pi = \sqrt{m_\pi^2 + p^2}$

$$S_{\rm B,F} = \int \frac{d^3p\, d^3x}{(2\pi\hbar)^3}\left[\pm(1\pm f)\ln(1\pm f) - f\ln f\right], \qquad f_\pi(E) = \frac{1}{\gamma_q^{-2} e^{E_\pi/T} - 1}.$$

Pion gas properties: ***N*-particle, *E*-energy, *S*-entropy, *V*-volume as function of γ_q.**

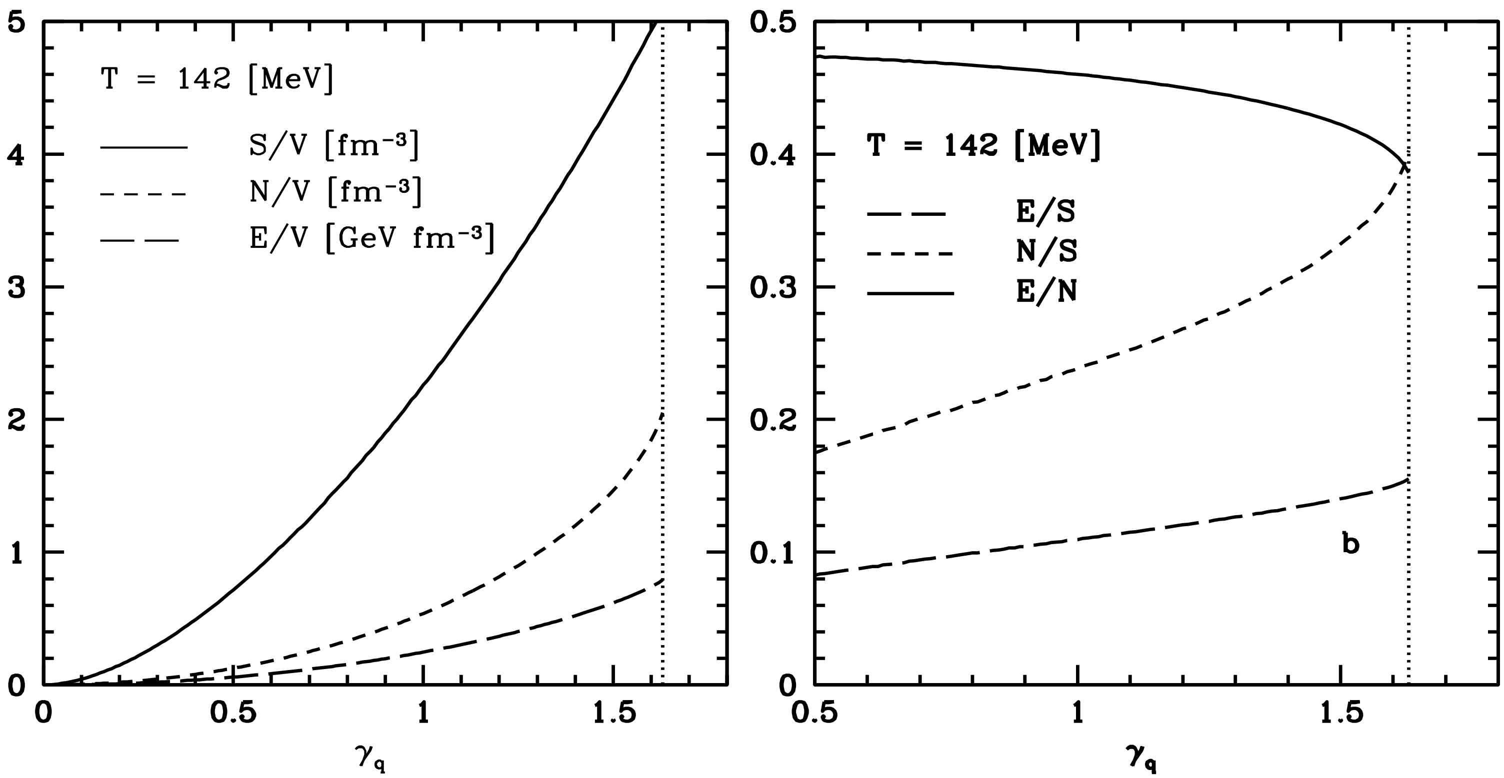

Entropy Conservation: QGP to hadron breakup at fixed volume and s

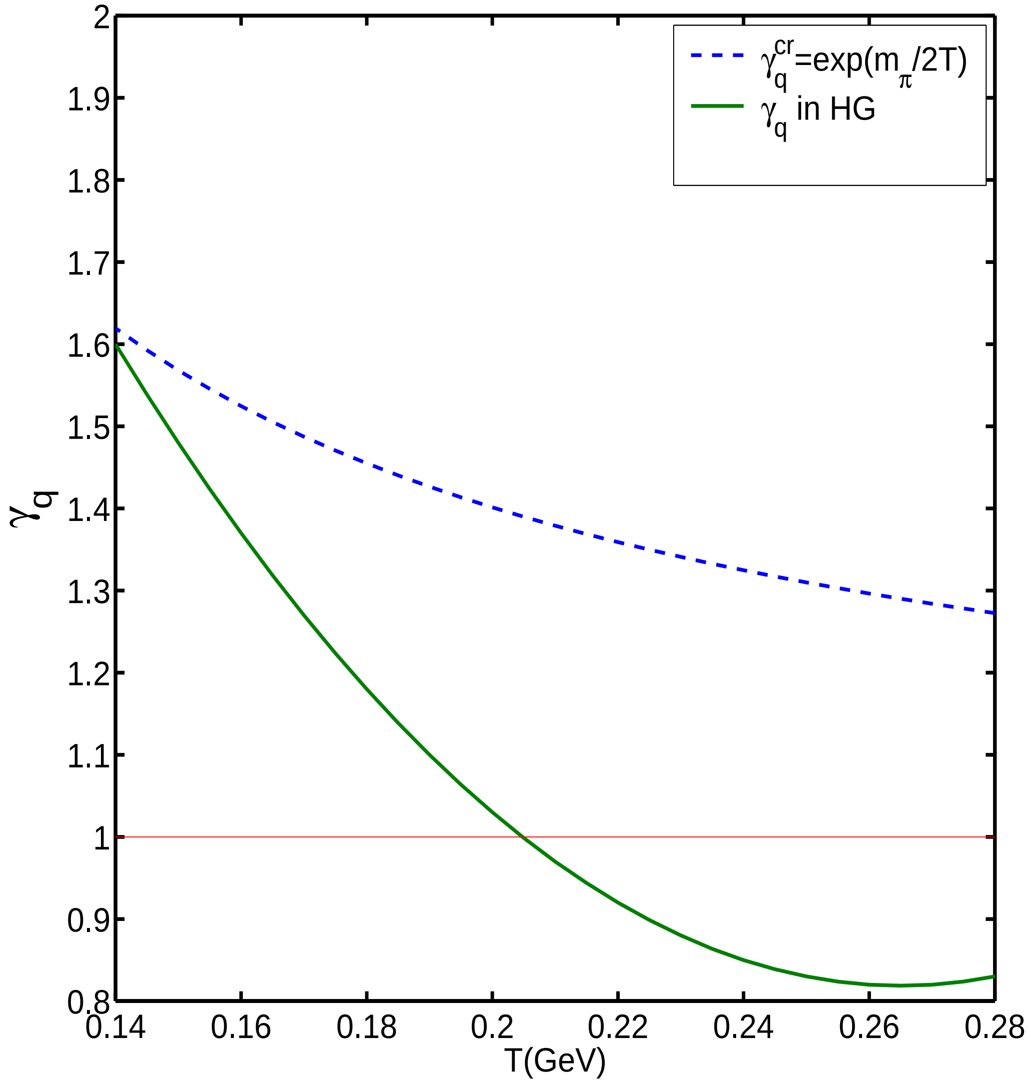

For $T > 205$ MeV entropy content of QGP inferior to HG. For $T < 205$ MeV to accommodate the entropy rich QGP breakup we need to over-saturate hadron yield.

γ_s **was chosen such that strangeness content is preserved as well.**

/eject

How big can γ_s be?

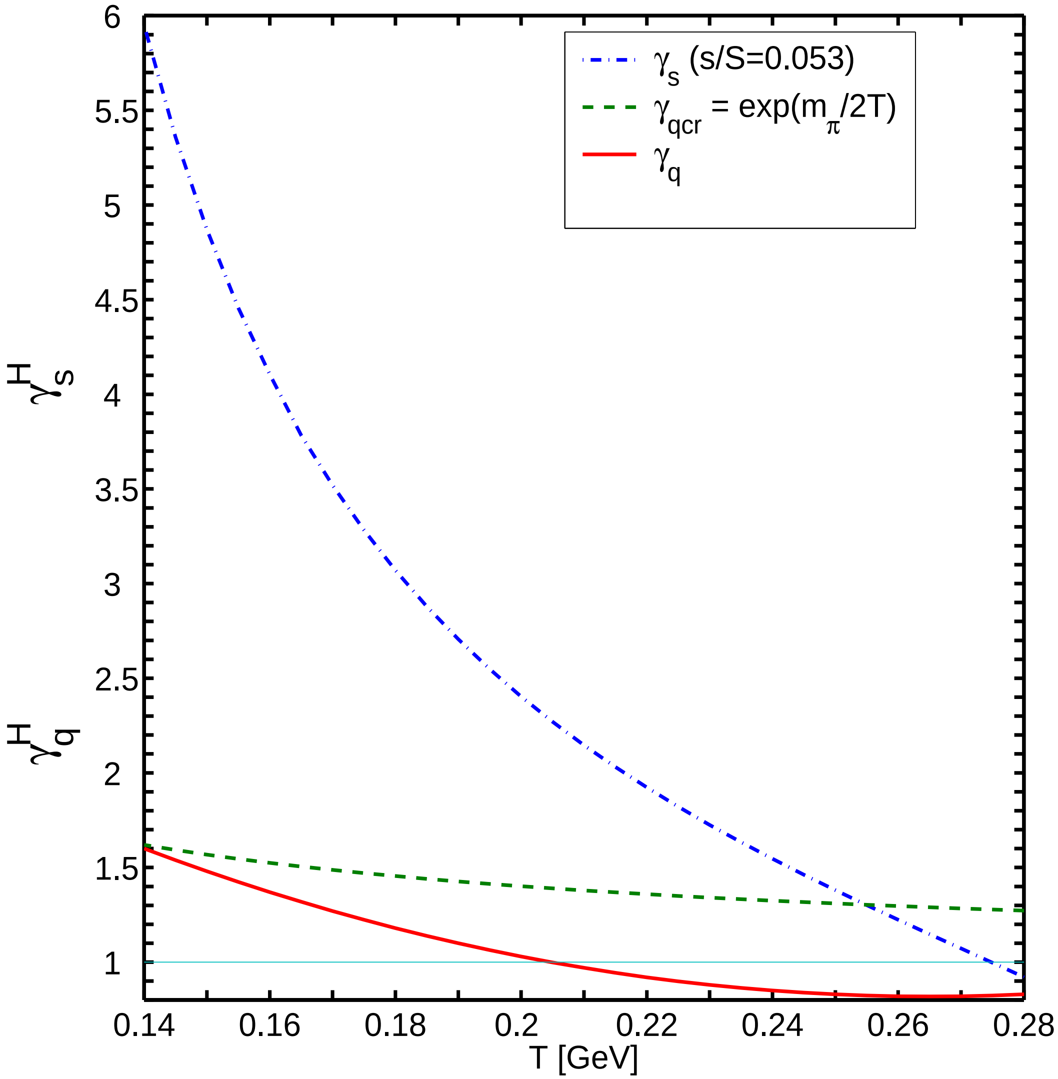

γ_q not visibly changed by taking QGP well above equilibrium. $\gamma_s^{\rm h}$ doubles!

/eject

Strangeness / Entropy in QGP

Relative s/S yield measures the number of active degrees of freedom and degree of relaxation when strangeness production freezes-out. Perturbative expression in chemical equilibrium:

$$\frac{s}{S}=\frac{\frac{g_s}{2\pi^2}T^3(m_s/T)^2K_2(m_s/T)}{(g2\pi^2/45)T^3+(g_s n_{\rm f}/6)\mu_q^2T}\simeq 0.028$$

much of $\mathcal{O}(\alpha_s)$ interaction effect cancels out

Allow for chemical non-equilibrium of strangeness $\gamma_s^{\rm QGP}$, and possible quark-gluon pre-equilibrium – gradual increase to the limit expected:

$$\frac{s}{S}=\frac{0.03\gamma_s^{\rm QGP}}{0.4\gamma_{\rm G}+0.1\gamma_s^{\rm QGP}+0.5\gamma_q^{\rm QGP}+0.05\gamma_q^{\rm QGP}(\ln\lambda_q)^2}\to 0.028.$$

We expect the yield of gluons and light quarks to approach chemical equilibrium fast and first: $\gamma_{\rm G}\to 1$ and $\gamma_q^{\rm QGP}\to 1$, thus $s/S\simeq 0.028\gamma_s^{\rm QGP}$.

CHECK: FIT YIELDS OF PARTICLES, EVALUATE STRANGENESS AND ENTROPY CONTENT AND COMPARE WITH EXPECTED RATIO,

•

1b. Statistical Hadronization

Hypothesis (Fermi, Hagedorn): particle production can be described by evaluating the accessible phase space.

Fermi: worked with hadron phase space, not a "hadron gas phase": for 'strong' interactions when all matrix elements are saturated ($|M|^2 \rightarrow 1$), rate of particle production according to the Fermi golden rule is the n-particle phase space. Micro canonical picture used by Fermi. With time begun to use (grand) canonical phase space, since number of particles and energy content sufficiently high (Hagedorn). When this happened some people forgot that: we are not necessarily working with a hadron matter phase, rather, we just emit particles into the hadron phase space. WE HADRONIZE THE QGP FIREBALL, nobody ever saw a hadron fireball at RHIC.

Verification of statistical hadronization:

Particle yields with same valance quark content are in relative chemical equilibrium, e.g. the relative yield of $\Delta(1230)/N$ as of K^*/K, $\Sigma^*(1385)/\Lambda$, etc, is controlled by chemical freeze-out i.e. Hagedorn Temperature $T_{\rm H}$:

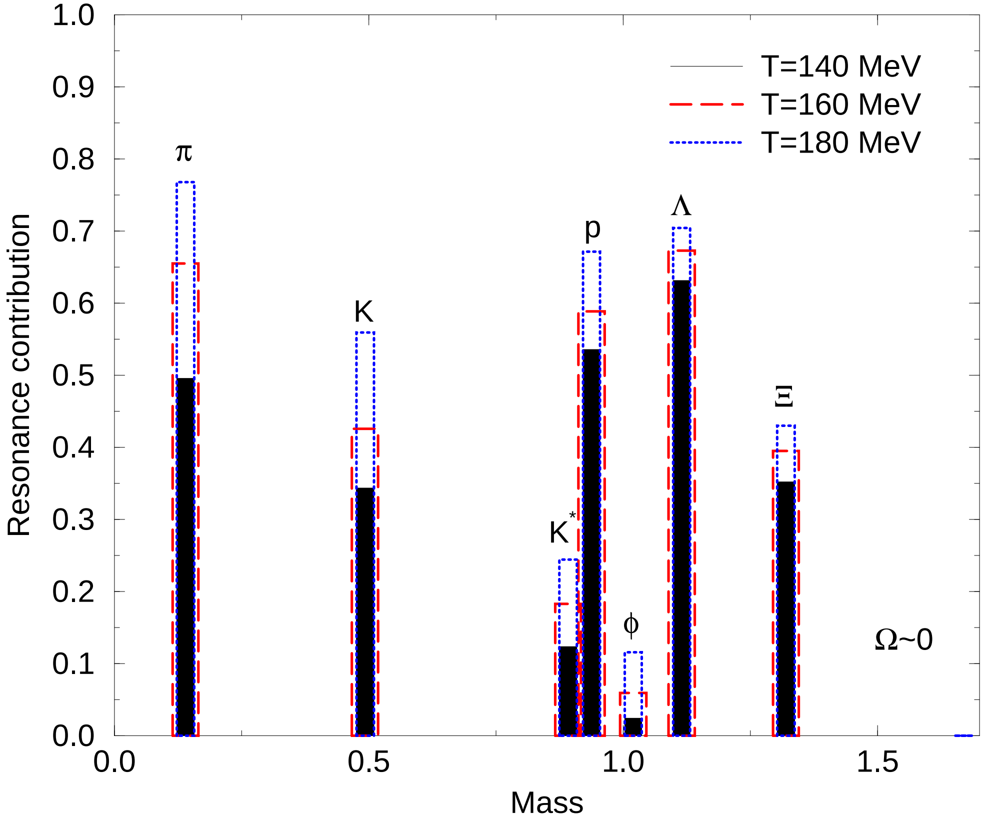

$$\frac{N^*}{N} = \frac{g^*(m^*T_{\rm H})^{3/2}e^{-m^*/T_{\rm H}}}{g(mT_{\rm H})^{3/2}e^{-m/T_{\rm H}}}$$

Resonances decay rapidly into 'stable' hadrons and dominate the yield of most stable hadronic particles.

Resonance yields test statistical hadronization principles. WE NEED MORE RESONANCE DATA

Resonances reconstructed by invariant mass; important to consider potential for loss of observability.

HADRONIZATION GLOBAL FIT:→

Counting particles

The counting of hadrons is conveniently done by counting the valence quark content $(u, d, s, \ldots \lambda_q^2 = \lambda_u \lambda_d,\ \lambda_{I3} = \lambda_u/\lambda_d)$:

$$\Upsilon_i \equiv \Pi_i \gamma_i^{n_i} \lambda_i^{k_i} = e^{\sigma_i/T}; \qquad \lambda_q \equiv e^{\frac{\mu_q}{T}} = e^{\frac{\mu_b}{3T}}, \qquad \lambda_s \equiv e^{\frac{\mu_s}{T}} = e^{\frac{[\mu_b/3-\mu_S]}{T}}$$

Example of NUCLEONS $\gamma_N = \gamma_q^3$**:**

$$\Upsilon_N = \gamma_N e^{\frac{\mu_b}{T}}, \qquad\qquad \Upsilon_{\overline{N}} = \gamma_N e^{\frac{-\mu_b}{T}};$$

$$\sigma_N \equiv \mu_b + T \ln \gamma_N, \qquad\qquad \sigma_{\overline{N}} \equiv -\mu_b + T \ln \gamma_N$$

Meaning of parameters from e.g. the first law of thermodynamics:

$$\begin{aligned} dE + P\,dV - T\,dS &= \sigma_N\,dN + \sigma_{\overline{N}}\,d\overline{N} \\ &= \mu_b(dN - d\overline{N}) + T \ln \gamma_N (dN + d\overline{N}). \end{aligned}$$

NOTE: For $\gamma_N \to 1$ **the pair terms vanishes, the** μ_b **term remains, it costs** $dE = \mu_B$ **to add to baryon number.**

•

2. Fits to Particle Yields: Example RHIC-200

Example we need: Fit of RHIC-200 as function of centrality, mostly non-strange hadrons. Implicit ab-initio prediction of multistrange baryons. Now if we are given dN/dy for similar bins of centrality we could even perform a global study.....

Statistical HAadronization with REsonsnces=SHARE

Full analysis of experimental hadron yield results requires a significant numerical effort in order to allow for resonances, particle widths, full decay trees, isospin multiplet sub-states.

Kraków-Tucson (NATO supported) collaboration produced a public package SHARE Statistical Hadronization with Resonances which is available e.g. at

http://www.physics.arizona.edu/˜torrieri/SHARE/share.html

Lead author: Giorgio Torrieri

With W. Broniowski, W. Florkowski, J. Letessier, S. Steinke, JR nucl–th/0404083 Comp. Phys. Com. 167, 229 (2005)

Online SHARE: Steve Steinke No fitting online (server too small)

http://www.physics.arizona.edu/˜steinke/shareonline.html

Aside of particle yields, also PHYSICAL PROPERTIES of the source are available, both in SHARE and ONLINE.

DATA: Centrality dependence of dN/dy for $\pi^{\pm}$, $K^{\pm}$, p and $\bar{p}$. The errors are systematic only. The statistical errors are negligible. PHENIX data

N_{part}	π^+	π^-	K^+	K^-	p	$\bar{p}$
351.4	**286.4 ± 24.2**	**281.8 ± 22.8**	**48.9 ± 6.3**	**45.7 ± 5.2**	**18.4 ± 2.6**	**13.5 ± 1.8**
299.0	**239.6 ± 20.5**	**238.9 ± 19.8**	**40.1 ± 5.1**	**37.8 ± 4.3**	**15.3 ± 2.1**	**11.4 ± 1.5**
253.9	**204.6 ± 18.0**	**198.2 ± 16.7**	**33.7 ± 4.3**	**31.1 ± 3.5**	**12.8 ± 1.8**	**9.5 ± 1.3**
215.3	**173.8 ± 15.6**	**167.4 ± 14.4**	**27.9 ± 3.6**	**25.8 ± 2.9**	**10.6 ± 1.5**	**7.9 ± 1.1**
166.6	**130.3 ± 12.4**	**127.3 ± 11.6**	**20.6 ± 2.6**	**19.1 ± 2.2**	**8.1 ± 1.1**	**5.9 ± 0.8**
114.2	**87.0 ± 8.6**	**84.4 ± 8.0**	**13.2 ± 1.7**	**12.3 ± 1.4**	**5.3 ± 0.7**	**3.9 ± 0.5**
74.4	**54.9 ± 5.6**	**52.9 ± 5.2**	**8.0 ± 0.8**	**7.4 ± 0.6**	**3.2 ± 0.5**	**2.4 ± 0.3**
45.5	**32.4 ± 3.4**	**31.3 ± 3.1**	**4.5 ± 0.4**	**4.1 ± 0.4**	**1.8 ± 0.3**	**1.4 ± 0.2**
25.7	**17.0 ± 1.8**	**16.3 ± 1.6**	**2.2 ± 0.2**	**2.0 ± 0.1**	**0.93 ± 0.15**	**0.71 ± 0.12**
13.4	**7.9 ± 0.8**	**7.7 ± 0.7**	**0.89 ± 0.09**	**0.88 ± 0.09**	**0.40 ± 0.07**	**0.29 ± 0.05**
6.3	**4.0 ± 0.4**	**3.9 ± 0.3**	**0.44 ± 0.04**	**0.42 ± 0.04**	**0.21 ± 0.04**	**0.15 ± 0.02**

In addition we use STAR data on $\mathrm{K}^*(892)/\mathrm{K}^-$, **and** ϕ/K^- **relative yields - these ratios are nearly constant as function of centrality**

Fits are ‘perfect’, there is no point presenting data tables how the yields agree. more important is to worry about the data values for the unstable particle input.

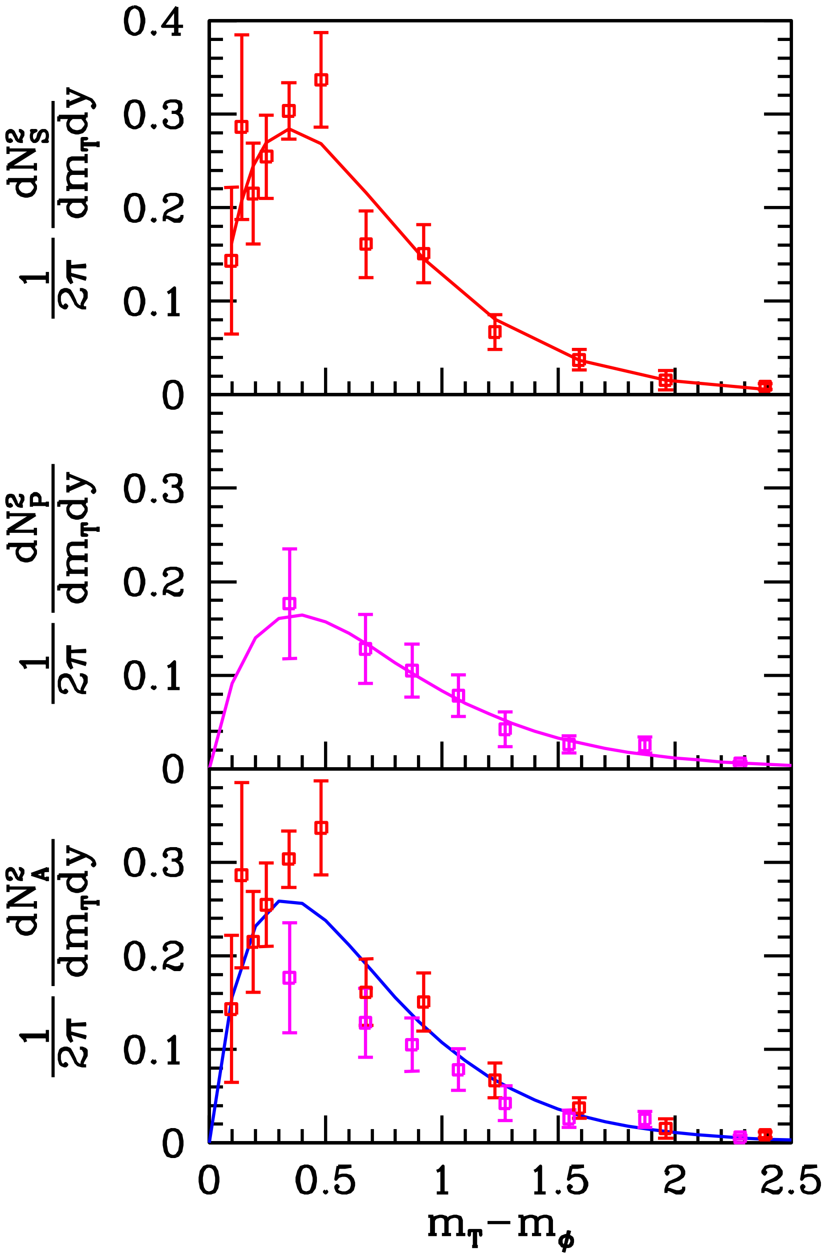

Include STAR data on $\mathrm{K}^*(892)/\mathrm{K}^-$**, and** ϕ/K^- **relative yields, these help decisively fix** γ_s ($\phi \propto \gamma_s^2$) **and** $T : Y \propto m^{3/2} e^{-m/T}$ **for** $m >> T$**.**

We considered the difference between STAR and PHENIX ϕ **yields. The lines show our best fit results to STAR (top panel), PHENIX (middle panel) and combined data set (bottom panel). The integrated yields agree for the top two panels with those reported by the experimental collaborations. We note that the integrated yield derived from the combined data fit (bottom panel), to all available 10% centrality** ϕ**-yields, is not compatible with the PHENIX yield. This is so, since the evaluation of the integrated PHENIX** ϕ**-yield depends on the lowest** $m_\perp$ **measured yield. This data point appears to be a 1.5 s.d. low anomaly compared to the many STAR** ϕ**-results available at low** $m_\perp$**. This possibly statistical fluctuation materially influences the total integrated PHENIX** ϕ**-yield.**

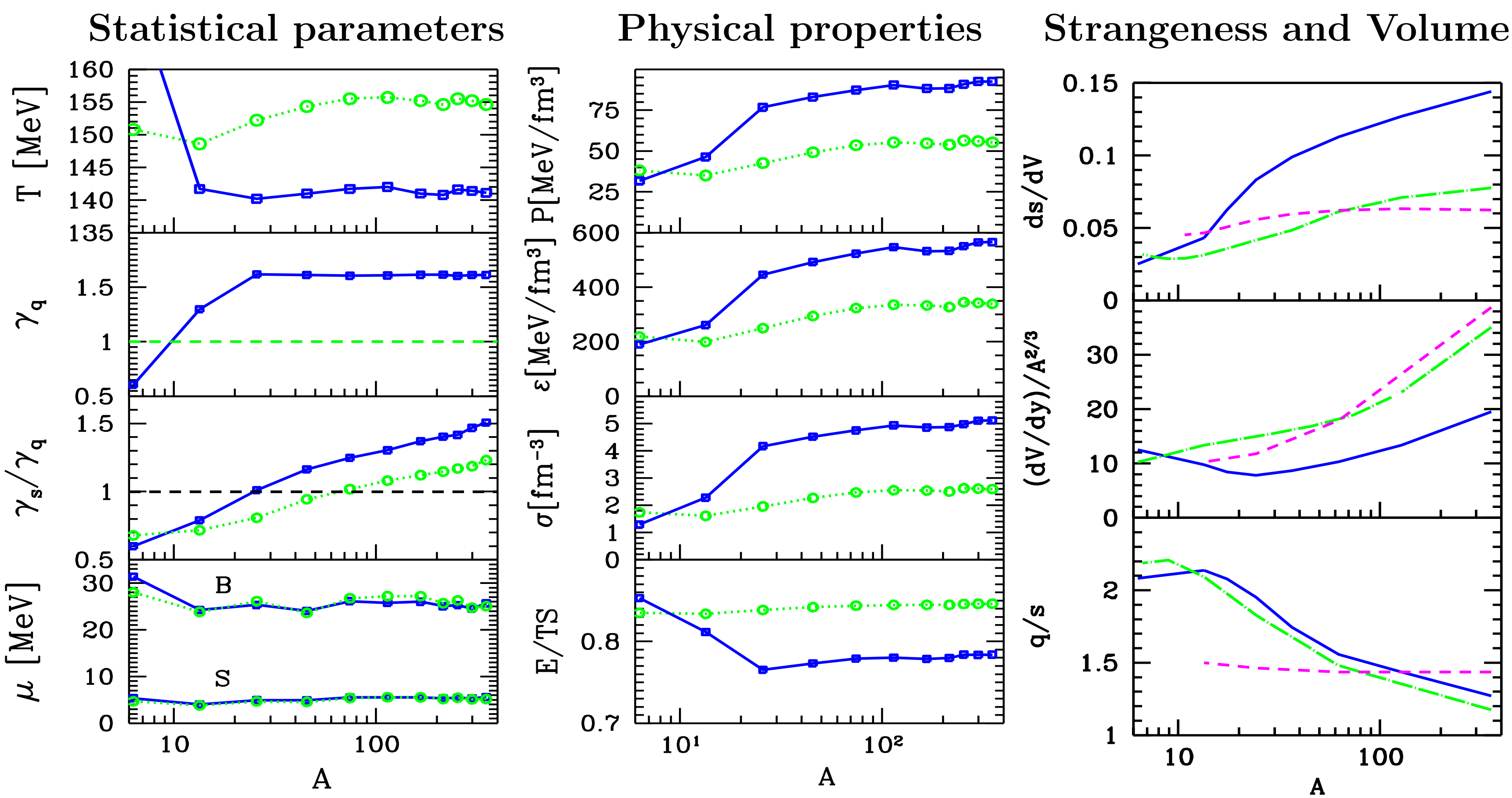

LINES: blue: nonequilibrium $\gamma_s, \gamma_q \neq 1$ and green semi-equilibrium $\gamma_s \neq 1, \gamma_q = 1$, $\gamma_s = \gamma_q = 1$

Highlights: γ_q changes with $A \propto V$ from under-saturated to over-saturated value,
$\gamma_s^{\rm HG}$ increases steadily to 2.4, implying near saturation in QGP.
P, σ, ϵ increase by factor 2–3, at $A > 20$ (onset of new physics?),
E/TS decreases with A - test of EoS.
Geometric transverse size scaling.
Strangeness grows faster than light quark yield (nonequilibrium) and hadronization density of strangeness increases with A.

Statistical + fit errors are seen in fluctuations, systematic error impacts absolute normalization by $\pm 10\%$.

RHIC200 PREDICTION OF dependence on centrality

Values of REFERENCE yields which define 1 do not alter Th/Ex-agreement

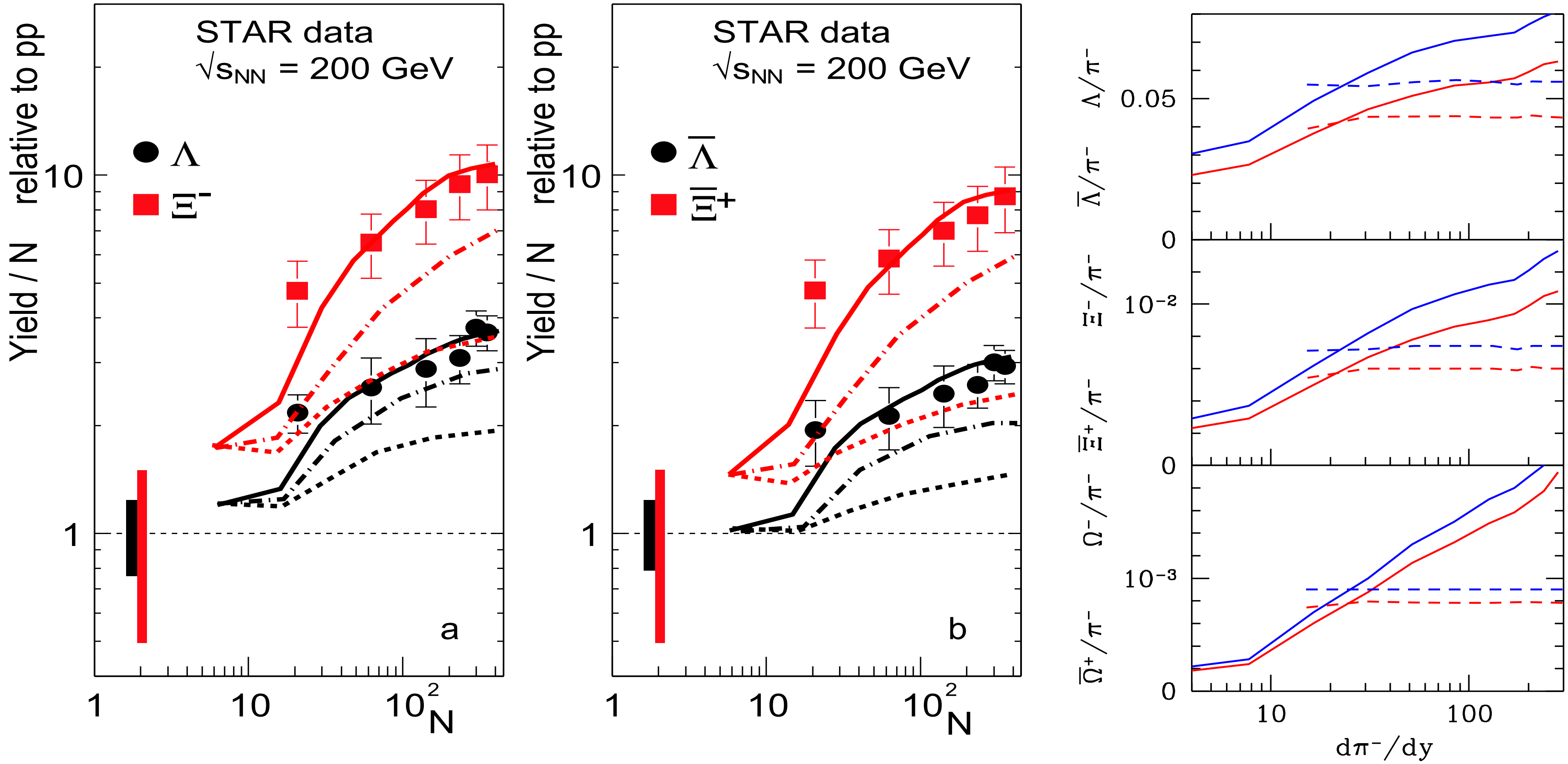

STAR $\sqrt{s_{\rm NN}} = 200$ GeV yields of hyperons $d\Lambda/dy$ and $d\Xi^-/dy$, (a), and antihyperons $d\overline{\Lambda}/dy$ and $d\overline{\Xi}^+/dy$, (b), normalized with, and as function of, A, relative to these yields in pp reactions: $d(\Lambda+\overline{\Lambda})/dy = 0.066 \pm 0.006$, $d(\Xi^- + \overline{\Xi}^+)/dy = 0.0036 \pm 0.0012$, $\overline{\Lambda}/\Lambda = 0.88 \pm 0.09$ and $\overline{\Xi}^+/\Xi^- = 0.90 \pm 0.09$. Solid lines, chemical non-equilibrium, dashed chemical equilibrium, (dash-dotted lines, semi-equilibrium.) On right, the predicted hyperons per π^- yields (blue for hyperons and for antihyperons).

s/b and s/S rise with increasing centrality $A \propto V$; E/s falls

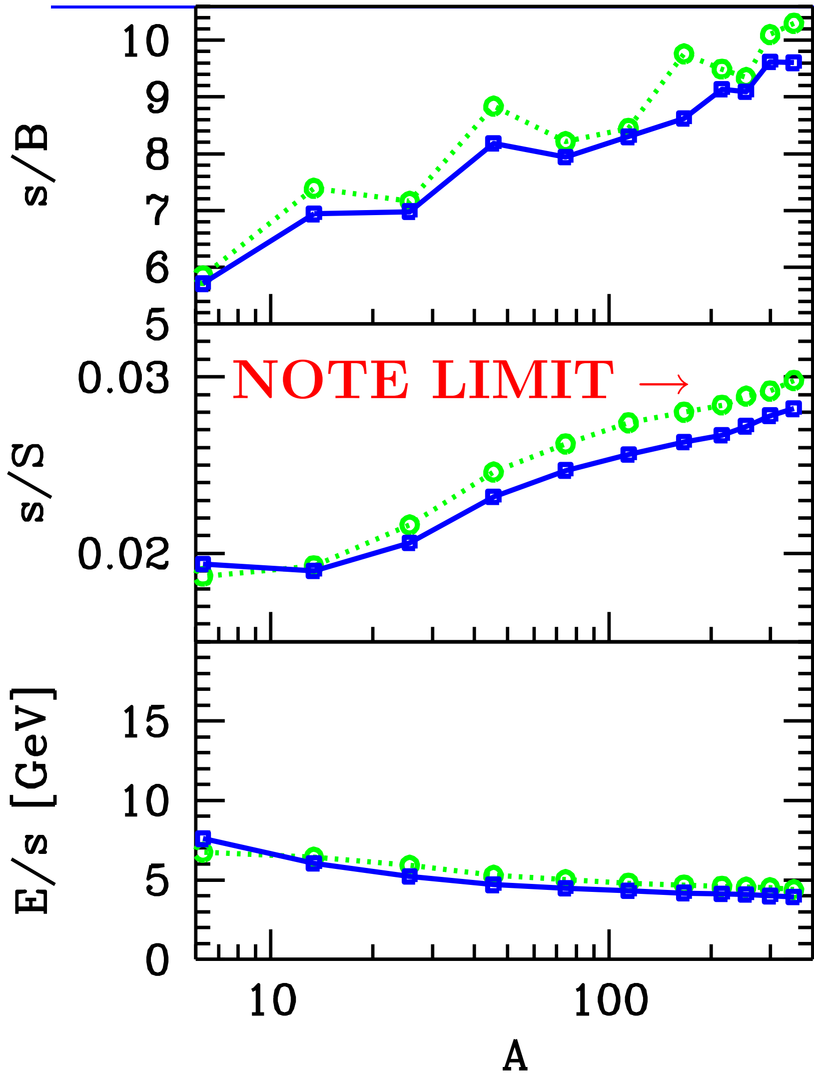

Showing results for both $\gamma_q, \gamma_s \neq 1$, for $\gamma_s \neq 1, \gamma_q = 1$. Note little difference in the result, even though the value of T will differ significantly.

1) $s/S \to 0.027$, as function of V;
2) most central value near QGP chemical equilibrium;
3) no saturation for largest volumes available;

Behavior is consistent with QGP prediction of steady increase of strangeness yield with increase of the volume, which implies longer lifespan and hence greater strangeness yield, both specific yield and larger $\gamma_s^{\rm QGP}$.

Agreement between nonequilibrium (blue) and semi-equilibrium (green, $\gamma_q = 1$) in description of bulk properties implies that MOST particle distributions extrapolate well from the experimental data - differences in e.g. $\Omega, \overline{\Omega}$ yields sensitive to the model issues do not impact bulk properties decisively.

•

3. Strangeness equilibration with fireball expansion

QCD allows to COMPUTE s/S and $\gamma_s^{\rm QGP}$
fine-tune at RHIC - extrapolate $\to$ LHC:

- **production of strangeness in gluon fusion** $\boxed{GG \to s\bar s}$
  strangeness linked to gluons from QGP;

dominant processes:

$$GG \to s\bar s$$

abundant strangeness =evidence for gluons

10–15% of total rate: $q\bar q \to s\bar s$

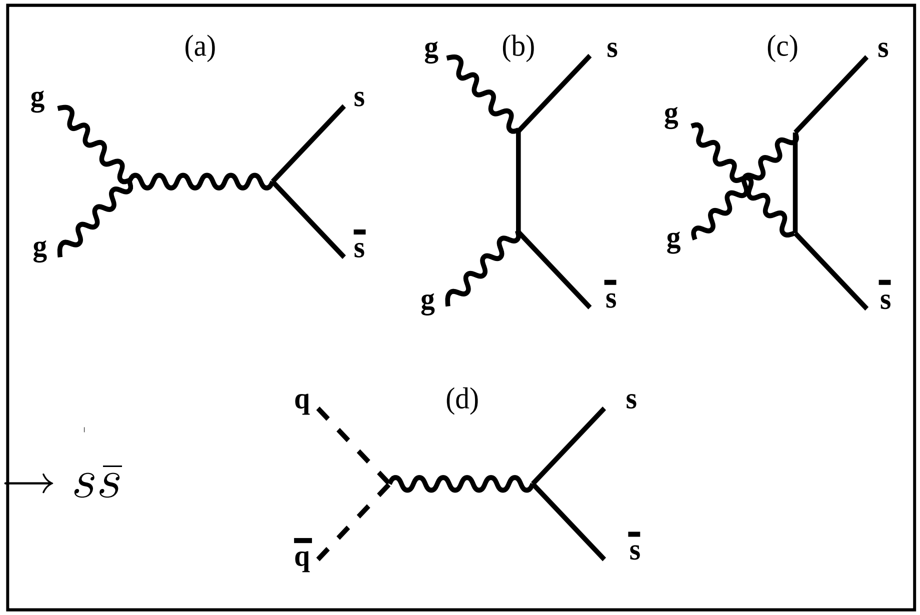

- **coincidence of scales:**

$$\boxed{m_s \simeq T_c} \to \boxed{\tau_s \simeq \tau_{\rm QGP}} \to$$

strangeness a clock for QGP phase

- $\boxed{\bar s \simeq \bar q} \to$ **strange antibaryon enhancement**
  at RHIC (anti)hyperon dominance of (anti)baryons.

Strangeness relaxation to chemical equilibrium

Strangeness density time evolution in local rest frame:

$$\frac{1}{V}\frac{ds}{d\tau} = \frac{1}{V}\frac{d\bar{s}}{d\tau} = \frac{1}{2}\rho_g^2(t)\,\langle\sigma v\rangle_T^{gg\to s\bar{s}} + \rho_q(t)\rho_{\bar{q}}(t)\langle\sigma v\rangle_T^{q\bar{q}\to s\bar{s}} - \rho_s(t)\,\rho_{\bar{s}}(t)\,\langle\sigma v\rangle_T^{s\bar{s}\to gg,q\bar{q}}$$

Evolution for s and $\bar{s}$ identical, which allows to set $\rho_s(t) = \rho_{\bar{s}}(t)$.
Note invariant production rate A and the characteristic time constant τ_s:

$$A^{12\to 34} \equiv \frac{1}{1+\delta_{1,2}}\gamma_1\gamma_2\rho_1^\infty\rho_2^\infty\langle\sigma_s v_{12}\rangle_T^{12\to 34}. \qquad 2\tau_s \equiv \frac{\rho_s(\infty)}{A^{gg\to s\bar{s}}+A^{q\bar{q}\to s\bar{s}}+\ldots}$$

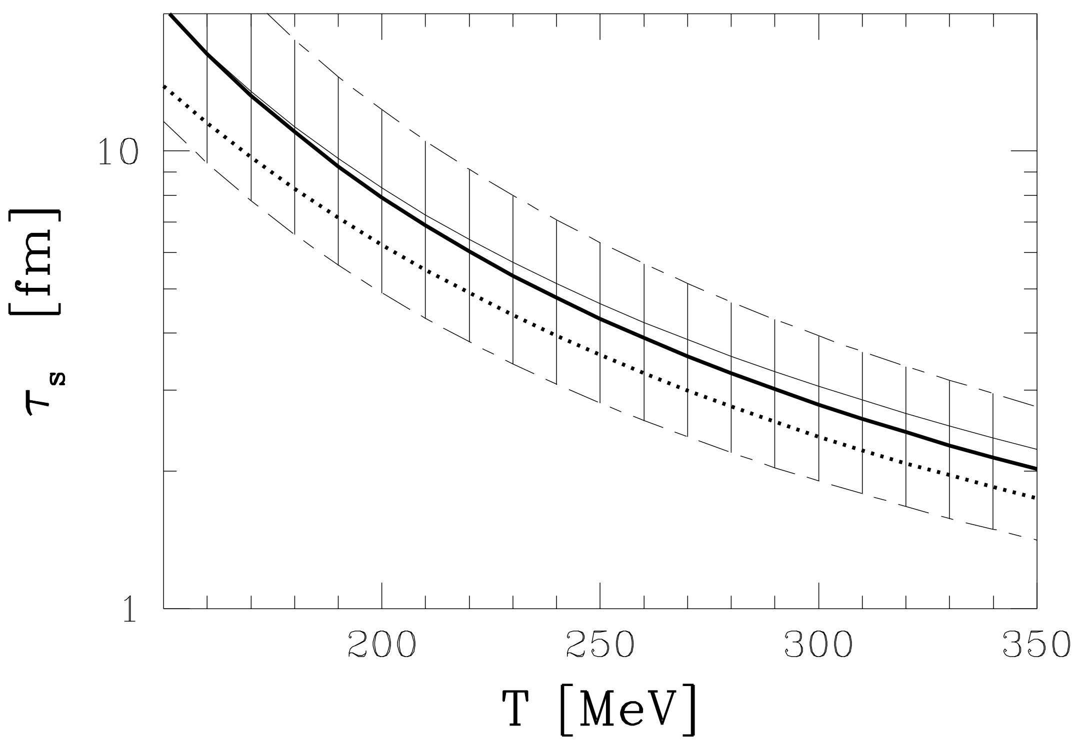

Thermal average rate of strangeness production

Kinetic (momentum) equilibration is faster than chemical, use thermal particle distributions $f(\vec{p}_1, T)$ to obtain average rate:

$$\langle \sigma v_{\rm rel} \rangle_T \equiv \frac{\int d^3p_1 \int d^3p_2 \sigma_{12} v_{12} f(\vec{p}_1, T) f(\vec{p}_2, T)}{\int d^3p_1 \int d^3p_2 f(\vec{p}_1, T) f(\vec{p}_2, T)} \, .$$

The generic angle averaged cross sections for (heavy) flavor s, $\bar{s}$ production processes $g + g \to s + \bar{s}$ and $q + \bar{q} \to s + \bar{s}$, are:

$$\bar{\sigma}_{gg \to s\bar{s}}(s) = \frac{2\pi\alpha_{\rm s}^2}{3s} \left[\left(1 + \frac{4m_{\rm s}^2}{s} + \frac{m_{\rm s}^4}{s^2}\right) \tanh^{-1} W(s) - \left(\frac{7}{8} + \frac{31 m_{\rm s}^2}{8s}\right) W(s) \right] ,$$

$$\bar{\sigma}_{q\bar{q} \to s\bar{s}}(s) = \frac{8\pi\alpha_{\rm s}^2}{27s} \left(1 + \frac{2m_{\rm s}^2}{s}\right) W(s) \, . \qquad W(s) = \sqrt{1 - 4m_{\rm s}^2/s}$$

RESUMMATION

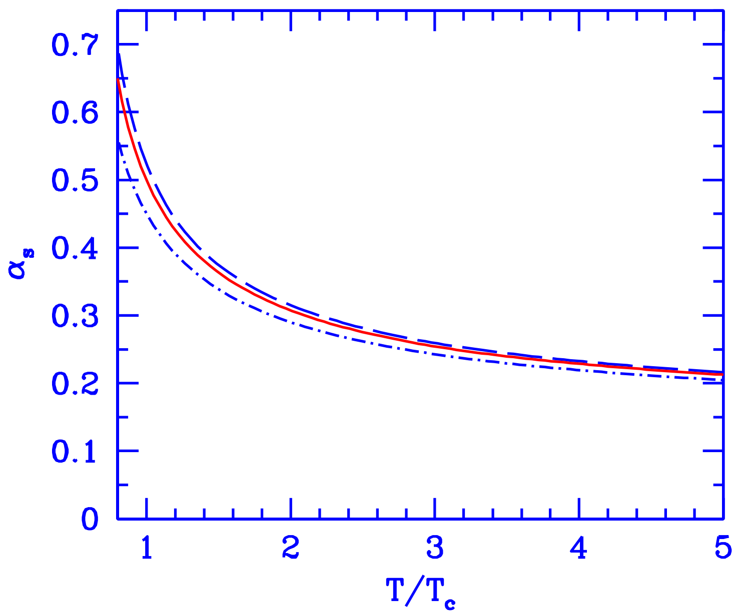

The relatively small experimental value $\alpha_{\rm s}(M_Z) \simeq 0.118$, established in recent years helps to achieve QCD resummation with running $\alpha_{\rm s}$ and $m_{\rm s}$ taken at the energy scale $\mu \equiv \sqrt{s}$.
Effective T-dependence:

$$\alpha_s(\mu = 2\pi T) \equiv \alpha_s(T) \simeq \frac{\alpha_s(T_c)}{1 + (0.760 \pm 0.002) \ln(T/T_c)}$$

with $\alpha_s(T_c) = 0.50 \pm 0.04$ and $T_c = 0.16$ GeV.
α_s^2 varies by factor 10

STRANGENESS IN ENTROPY CONSERVING EXPANSION

QGP expansion is adiabatic i.e. $(g_G = 2_s 8_c = 16, g_q = 2_s 3_c n_{\rm f})$

$$S = \frac{4\pi^2}{90} g(T) V T^3 = \textbf{Const.} \quad g = g_G\left(1 - \frac{15\alpha_s(T)}{4\pi} + \ldots\right) + \frac{7}{4} g_q \left(1 - \frac{50\alpha_s(T)}{21\pi} + \ldots\right)\ .$$

The volume, temperature change such that $\delta(gT^3V) = 0$**. Strangeness phase space occupancy,** $g_s = 2_s 3_c \left(1 - \frac{k\alpha_s(T)}{\pi} + \ldots\right), k = 2$ **for** $m_s/T \to 0$**:**

$$\gamma_s(\tau) \equiv \frac{n_s(\tau)}{n_s^\infty(T(\tau))}, \quad n_s(\tau) = \gamma_s(\tau) T(\tau)^3 \frac{g_s(T)}{2\pi^2} z^2 K_2(z), \quad z = \frac{m_s}{T(t)}, \quad K_i : \text{Bessel f.}$$

evolves due to production and dilution, keeping entropy fixed:

$$\frac{d}{d\tau}\frac{s}{S} = \frac{A_G}{S/V}\left[\gamma_{\rm G}^2 - {\gamma_s}^2\right] + \frac{A_q}{S/V}\left[\gamma_{\rm q}^2 - {\gamma_s}^2\right]$$

Which for γ_s **assumes the form that makes dilution explicit:**

$$\frac{d\gamma_s}{d\tau} + \gamma_s \frac{d \ln[g_s z^2 K_2(z)/g]}{d\tau} = \frac{A_G}{n_s^\infty}\left[\gamma_{\rm G}^2 - {\gamma_s}^2\right] + \frac{A_q}{n_s^\infty}\left[\gamma_{\rm q}^2 - {\gamma_s}^2\right]$$

For $m_s \to 0$ **dilution effect decreases, disappears, and** $\gamma_s \le \gamma_{G,q}$**, importance grows with mass of the quark,** $z = m_s(T)/T$**, which grows near phase transition boundary.**

Model of temporal evolution of Temperature

To integrate the equation for s/S we need to understand $T(\tau)$.

We have at our disposal the final conditions: $S(\tau_f)$, $T(\tau_f)$ and since particle yields $dN_i/dy = n_i dV/dy$ also the volume per rapidity, $\Delta V/\Delta y|_{\tau_f}$. Theory (lattice) further provides Equations of State $\sigma(T) = S/V$. Hydrodynamic expansion with Bjørken scaling implies STRICTLY $dS/dy = \sigma(T) dV/dy = \mathrm{Const.}$ as function of time.

$dV/dy(\tau)$ expansion completes the model. This allows to fix $T(\tau)$.

$$\frac{dV}{dy} = A_\perp(\tau) \left.\frac{dz}{dy}\right|_{\tau=\mathrm{Const.}} . \qquad \mathrm{Bjørken}: \; z = \tau \sinh y \;\; \rightarrow \left.\frac{dz}{dy}\right|_{\tau=\mathrm{Const.},y=0} = \tau$$

We consider two transverse expansion pictures: bulk and donut ($dscaleswithR_\perp$):

$$A_\perp = \pi R_\perp^2(\tau) \quad \text{or} \quad A_\perp = \pi \left[R_\perp^2(\tau) - (R_\perp^2(\tau) - d)^2\right]$$

We do assume gradual onset of expansion - hydro motivated:

$$v(\tau) = v_{\max} \frac{2}{\pi} \arctan[4(\tau - \tau_0)/\tau_v]$$

Values of $v_{\max}$ we consider are in the range of 0.5–0.8c, the relaxation time $\tau_c \simeq 0.5$ fm, and the onset of transverse expansion τ_0 was tried in range 0.1–1 fm.

We took $R_\perp(\tau_0) = 5\,$fm for 5% most central collisions. For centrality dependence, We further scale the initial entropy as function of centrality to assure $\frac{dS}{dy} \simeq 8(A^{1.1} - 1)$ which we found in the centrality data analysis.

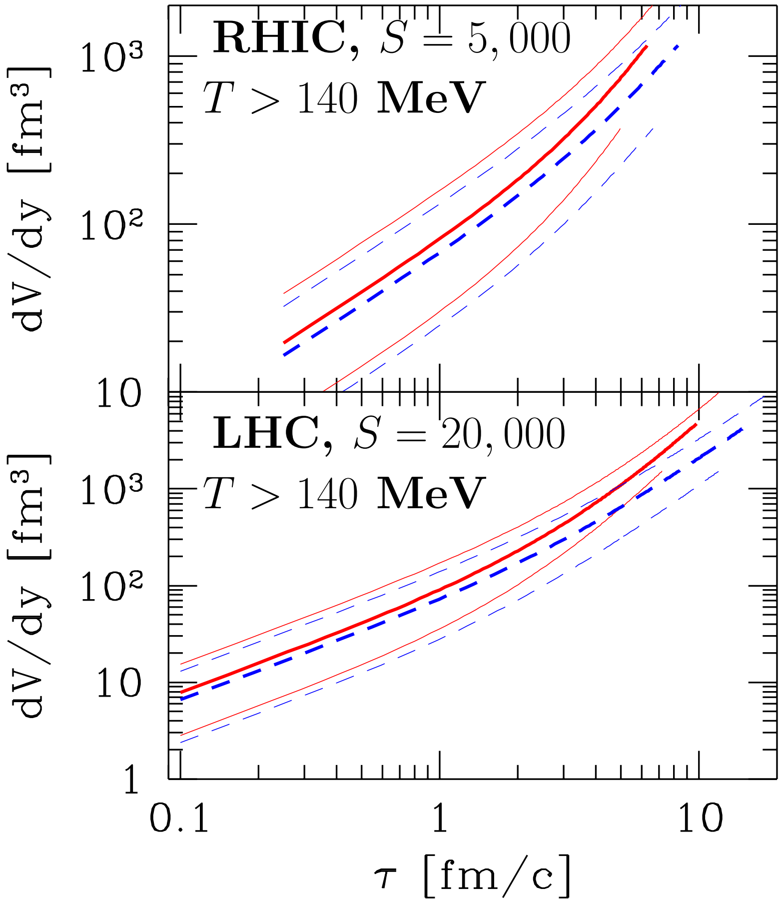

Three centralities: middle $R_\perp = 5$ fm and the upper/lower lines corresponding to $R_\perp = 7$, and, $R_\perp = 3$ fm/c. dashed lines for donut geometry $d = 2.1,\ 3.5$ and 4.9 fm.

Main difference LHC to RHIC, lifespan much longer, despite increase of average final expansion velocity from 0.6 to 0.8 c.

•

4. Centrality dependence of s/S at RHIC-200 and LHC

s/S and γ_s at RHIC: centrality dependence

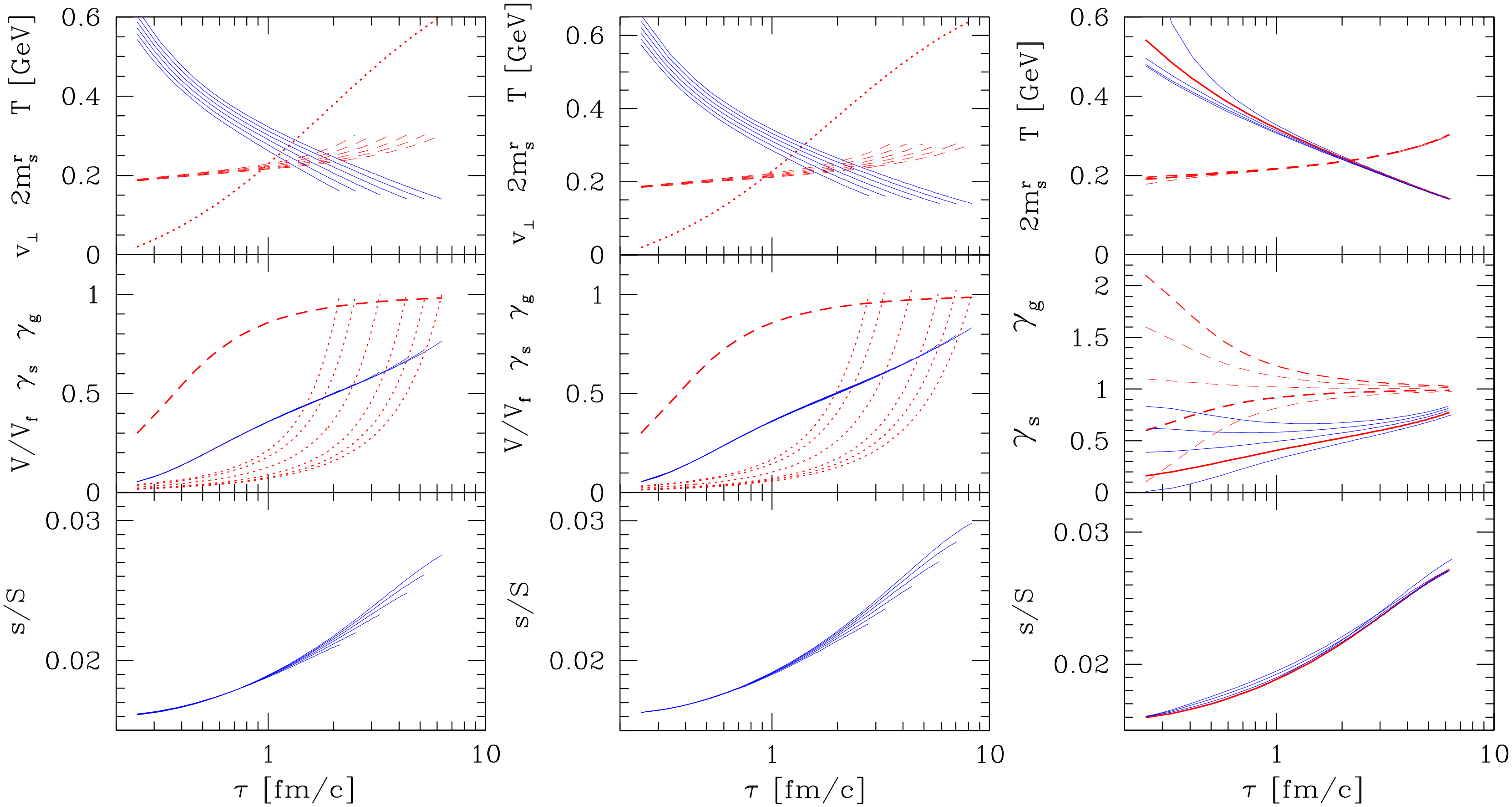

The two left panels: **Comparison of the two transverse expansion models, bulk expansion (left), and wedge expansion. Different lines correspond to different centralities. On right: study of the influence of the initial density of partons.**

Top: T**, middle** γ_s **and bottom** s/S

Assumptions:

dotted top panel: profile of $v_\perp(\tau)$**, the transverse expansion velocity; middle panel: dashed** $\gamma_g(\tau)$**,(which determines slower equilibrating** γ_q **dotted: normalized** $dV/dy(\tau)$ **normalized by the freeze-out value.**

What this means for LHC

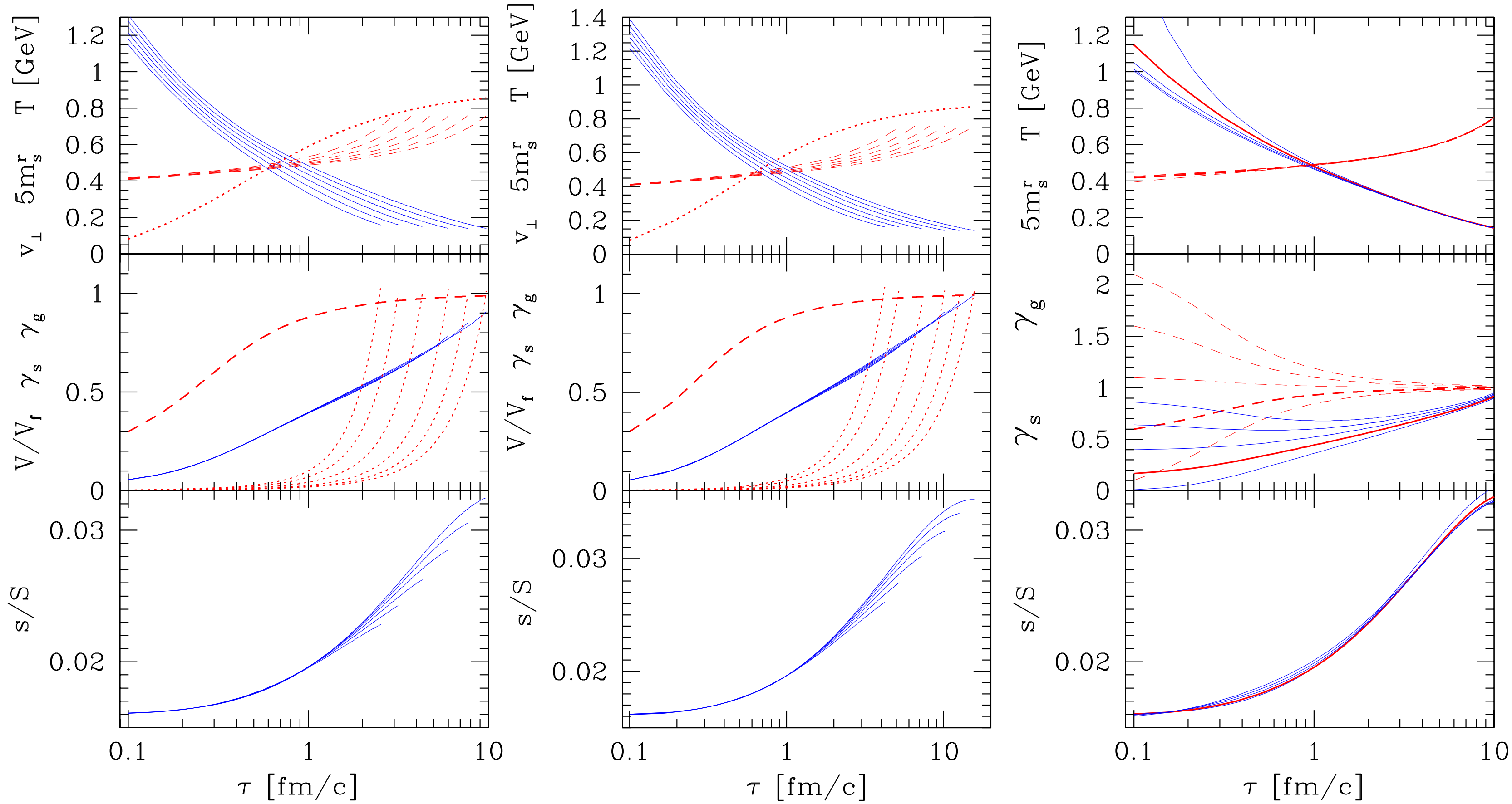

Comments (same LHC and RHIC:

Top Panel: Initial temperatures accommodate $dS/dy|_{\rm f}$ beyond participant scaling.

Middle Panel: Solid line(s): resulting γ_s for different centralities overlay;

Bottom panel: resulting s/S for different centralities, with R_0 stepped down for each line by factor 1.4.

Notable LHC differences to RHIC: (we assumed $dS/dy|_{\rm LHC} = 4dS/dy|_{\rm RHIC}$)

- **There is a significantly longer expansion time to the freeze-out condition (factor 2).**
- **There is a 20% growth in s/S**
- **There is a significant increase in initial temperature to accommodate increased entropy density.**

Strange quark mass matters

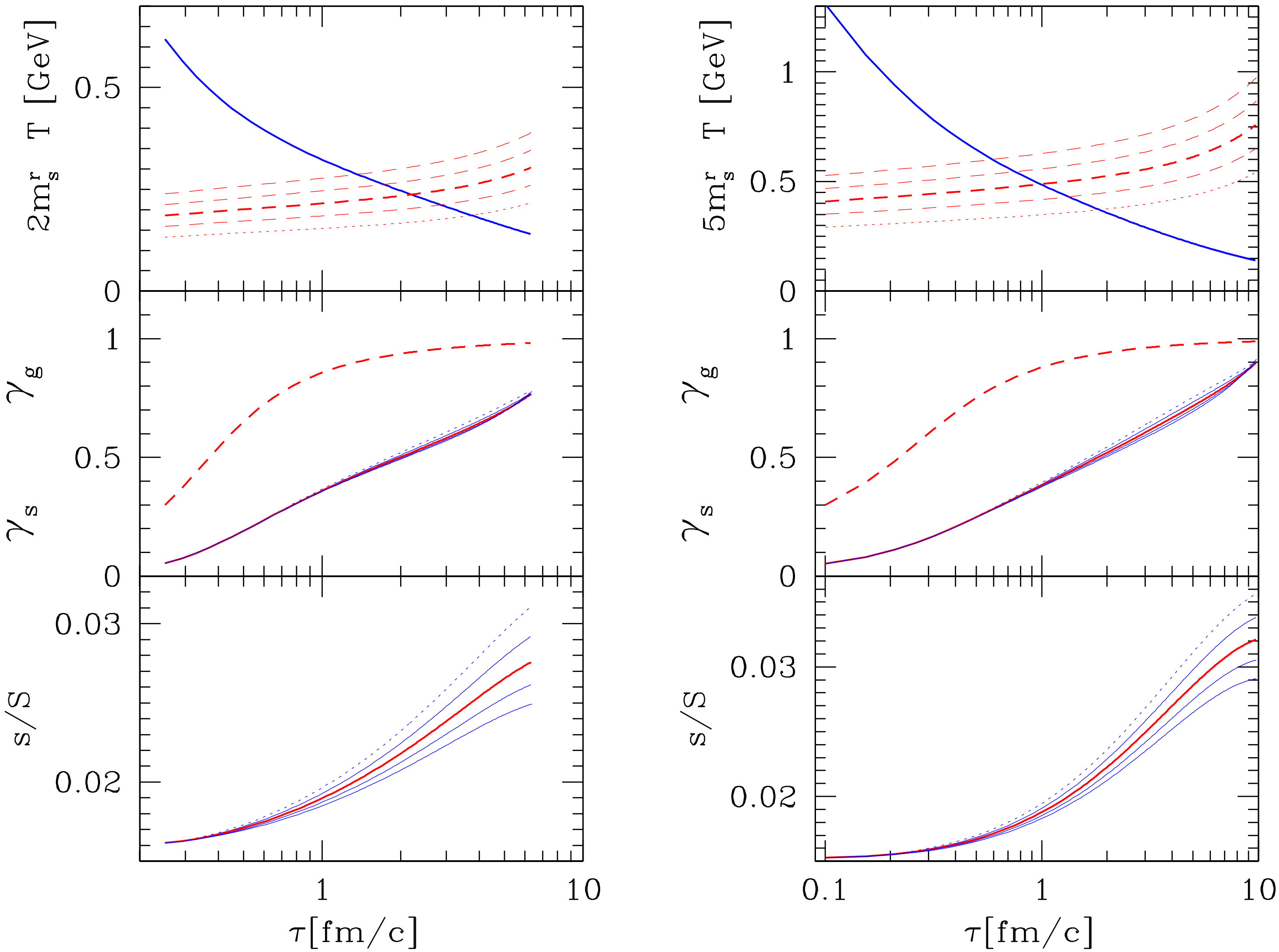

Left RHIC, right LHC, bulk volume expansion. m_s varies by factor 2.

γ_s overlays: Accidentally two effects cancel: for smaller mass more strangeness production, but by definition γ_s smaller. s/S of course bigger for smaller mass.

A first look at energy dependence

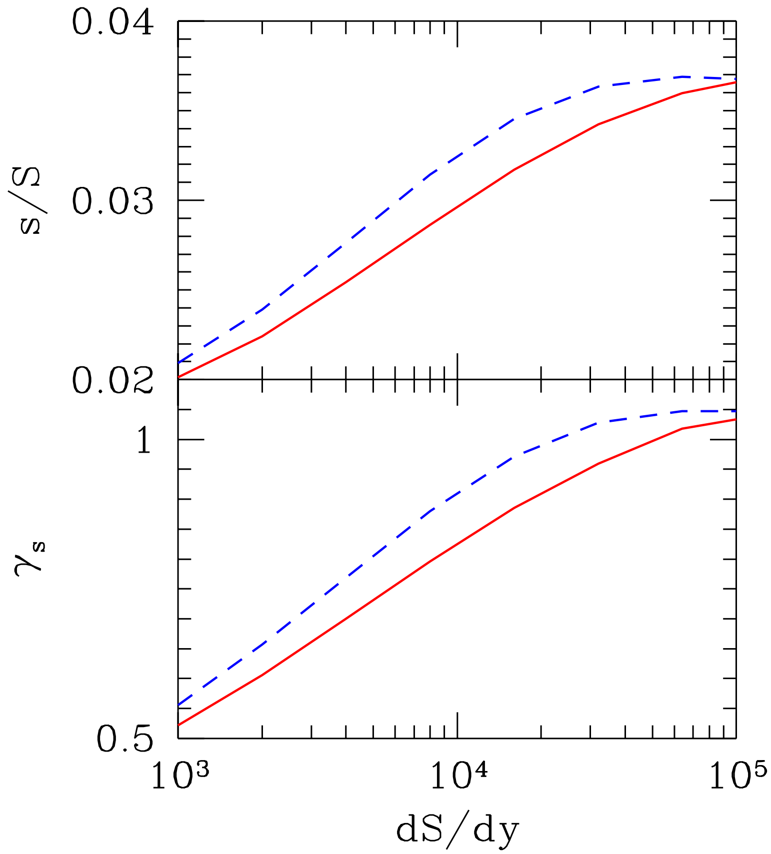

Solid, bulk expansion, dashed donut expansion.

Since the main parameter controlling the reaction energy dependence is the value of entropy (hadron multiplicity) produced, and we already have two points dS/dy=5,000 and 20,000 (LHC) we complete for central collisions the results.

QGP equilibrates gradually, some over-equilibration for large entropy content.

•

5. Soft (strange) hadrons at RHIC and LHC

For orientation: relationship of multiplicity to dS/dy

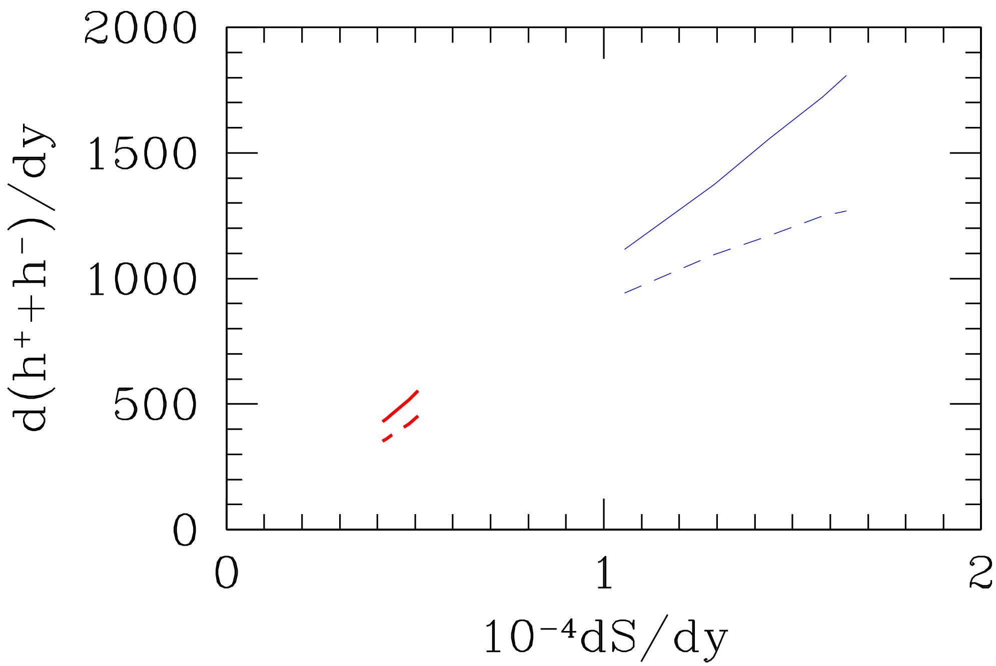

The yield of charged hadrons $d(h^- + h^+)/dy$ for different values of dS/dy. Solid lines: after all weak decays, dashed lines: before weak decays. Left domain for RHIC and right domain for LHC - defined at $E/b = 40, 412$ GeV respectively,obtained not as fit to data but assuming $E/TS = 0.78$, baryon conservation etc. See: hep-ph/0506140 and Eur. Phys. J. C (2005) -02414-7 by JR and JL "Soft hadron ratios at LHC"

How much enhancement in from RHIC to LHC K/π ?

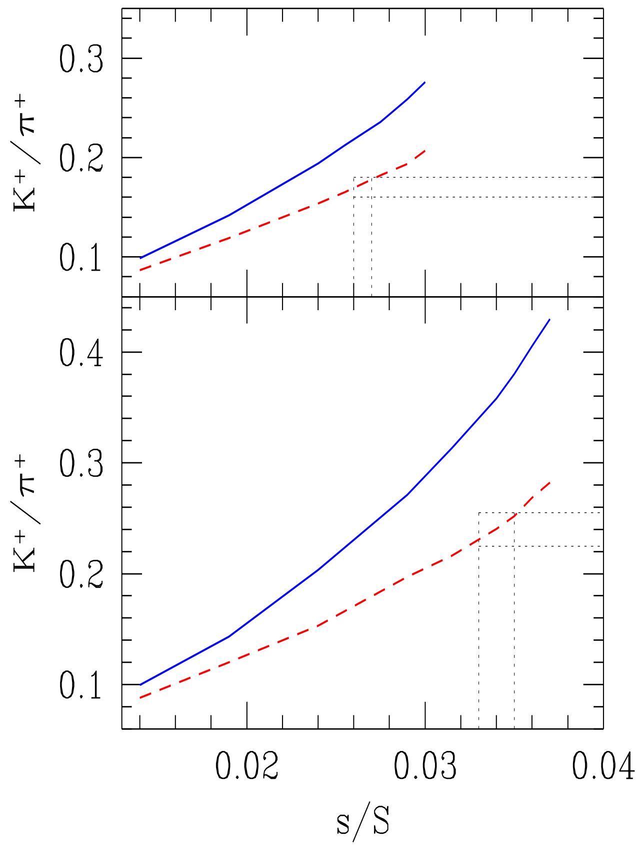

K^+/π^+ ratio as function of attained specific strangeness at freeze-out, s/S. Solid lines bare yields, dashed lines after all weak decays have diluted the pion yields. Top for RHIC and bottom for LHC physics environment. An increase by about 40% is predicted from $K^+/\pi^+ = 0.17$ at RHIC to $K^+/\pi^+ = 0.24$ at LHC. If LHC is subject to donut-expansion, increase more significant.

Multi strange hadrons are more sensitive to s/S

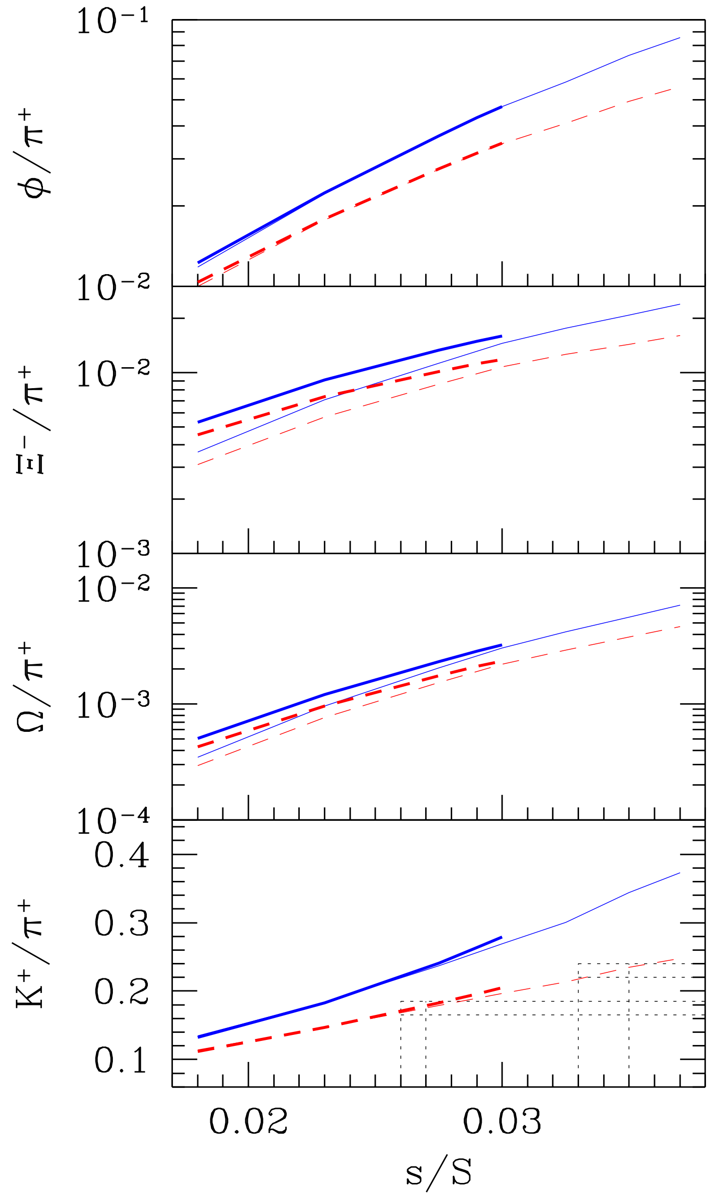

Top three panels: Φ/π^+, Ξ^-/π^+, Ω^-/π^+ **(log scale) relative yields of multistrange hadrons, as function of** s/S Φ/π^+, Ξ^-/π^+, Ω^-/π^+ **(log scale).**

Solid lines primary relative yields, dashed lines after all weak decays. Thick line with $s/S < 0.3$ **are for RHIC and thin lines are for LHC physics environment.**

Bottom panel: restating for comparison K^+/π^+.

6. Conclusions

- **Convincing evidence for CHEMICAL equilibration of the QGP, not final state hadrons: which abundances are controlled by prevailing valance quark yields and are not in chemical equilibrium;**
- **RHIC-200 results for K, ϕ, K* and non-strange hadrons as function of centrality produce impact parameter dependence of QGP observables which agrees with ...**
- **...QCD based evaluation of the two QGP global observables γ_s and s/S produces strangeness enhancement – additional strangeness beyond initial state. Enhancement by a factor 1.6-2.2 for s/S seen.**
- **Physical properties at Freeze-out such as $E/TS, E/b$ can be extrapolated across energy range and allow prediction of LHC particle yields;**
- **QCD kinetic model tuned to describe strangeness at RHIC, predicts further increase of specific enhancement at LHC with strong additional enhancement of multistrange hadrons and some noticeable increase in K$^+/\pi^+$.**